

Generalized PolyCube Trivariate Splines

Bo Li
SUNY Stony Brook

Xin Li
Louisiana State University

Kexiang Wang
SUNY Stony Brook

Hong Qin
SUNY Stony Brook

Abstract—This paper develops a new trivariate hierarchical spline scheme for volumetric data representation. Unlike conventional spline formulations and techniques, our new framework is built upon a novel parametric domain called Generalized PolyCube (GPC), comprising a set of regular cubes being glued together. Compared with the conventional PolyCube (PC) that could serve as a “one-piece” 3-manifold domain, GPC has more powerful and flexible representation ability. We develop an effective framework that parameterizes a solid model onto a topologically equivalent GPC domain, and design a hierarchical fitting scheme based on trivariate T-splines. The entire data-spline-conversion modeling framework provides high-accuracy data fitting and greatly reduce the number of superfluous control points. It is a powerful toolkit with broader application appeal in shape modeling, engineering analysis, and reverse engineering.

Keywords-Trivariate Spline; Generalized PolyCube; Volumetric Parameterization.

I. INTRODUCTION

The engineering design industry frequently pursues data conversion from discrete 3D data to compact and continuous spline formulations in scientific computing and industrial applications (e.g., reverse engineering). Compared with surface splines, trivariate splines can represent both boundary shape and real volumetric physical/material attributes. This is vital and highly desirable in many physically-based applications including mechanical analysis [4], physically-based shape editing, virtual-surgery training, etc.

To model an arbitrary 3-D manifold using conventional trivariate splines, current approaches decompose the model to many simple solid primitives first, and then design trivariate spline representations for each sub-region respectively. Separate splines must glue together along shared boundaries in order to ensure continuity of certain degree. For models with non-trivial topology and complicated geometry, the entire partitioning and patching/gluing process is primarily performed manually, and it requires intensive labor from users with domain knowledge. To overcome this difficulty in modeling general data, we forge ahead with our research efforts in PolyCube mapping, and construct the trivariate splines over the volumetric Generalized PolyCube (GPC) domain. The solid PolyCube-shaped domain is regular and offers a cuboid structure. It has many advantages over other parametric domains (See Table II and Section IV for more discussions) and is ideal for trivariate spline construction.

In this paper, we design algorithms to construct trivariate T-splines over GPC for general volumetric data and demonstrate their efficacy as the global “one-piece” representation with hierarchical fitting capability.

Contribution and Overview. The main contributions of this work include:

- (1) We develop an effective framework to compute the Generalized PolyCube (GPC) parameterization. Compared with the conventional PC, GPC is a more natural parametric domain to represent 3-manifolds with complicated topology.
- (2) We present a global “one-piece” trivariate spline scheme without stitching/trimming for general volumetric models. GPC provides parametric representation for topologically-complex models using very few cubes.
- (3) We design an efficient trivariate T-spline fitting algorithm, that supports hierarchical refinement with improved accuracy and reduced number of control points.

II. GENERALIZED POLYCUBE

A global one-piece parametric representation for shape with nontrivial topology is highly desirable for many geometric modeling and processing tasks, because it prevents artifacts caused by stitching/trimming over shared boundaries of solid primitives. The *PolyCube* representation is of particular interest toward this ambitious goal since it has perfect local regularity (i.e., local homogeneity) for tensor-product spline design. The idea of parameterizing a shape onto a conventional PolyCube (PC) is introduced by Tarini et al. [9]. A PolyCube is glued by a set of unit cubes. Therefore, consistent sets of knot intervals can be devised on a PolyCube straightforwardly. PolyCube parameterization has been studied by different researchers for various shape modeling tasks [9], [10]. In this work, we propose a novel concept called *Generalized PolyCube* (GPC), where the gluing direction of two faces shall be explicitly identified and a cube is even allowed to glue to itself (see Section II-A for details). Moreover, cube primitives are not enforced to have a true 3D embedding with principal axis alignment. In essence, a GPC domain consists of a set of cubes with connectivity information.

What inspires the design of GPC is that not all volumetric data can be parameterized effectively by PC. Figure 1 illustrates some examples. If we look at a solid torus ($S^1 \times D^2$) (a), topologically, the most concise representation is simply a cube with two opposite sides glued together (b); geometrically, the number of cubes required for low-distorted parameterization is related to the shape of the torus. However, a commonly-used PC representation typically requires eight cubes (c) to form a handle. Furthermore, if the solid torus is twisted, like a solid Möbius band (d), conventional PC can no longer

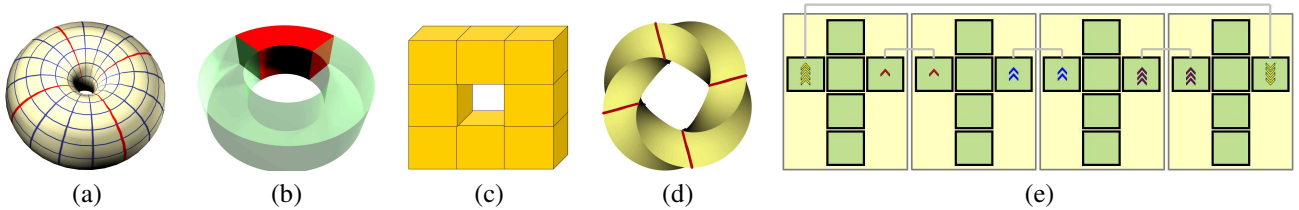


Figure 1: PolyCube (PC) vs Generalized PolyCube (GPC). A solid torus (a) is topologically equivalent to a cube with two opposite faces glued together (b), but in PC representation it needs at least eight cubes to comprise a handle. The twisted shapes such as a thick Möbius band (d) cannot be effectively represented by PC, yet can be easily represented in GPC, (e) shows the corresponding GPC-graph.

encode such information in any intuitive means. In contrast, GPC affords an efficient intrinsic representation of these shapes to intuitively encode topology of 3-manifolds correctly, while generally using far fewer cubes than PC as well. As a parametric domain that is both intrinsic and homogeneous, the GPC may not have a real global embedding in \mathbb{R}^3 , but it indeed offers a local embedding for each cube primitive, and therefore, sufficiently serves as a desirable parametric domain for trivariate spline construction.

A. GPC and GPC-Graph

The global structure of a Generalized PolyCube can be abstracted in a graph, which we call it a *GPC-graph*. Each node of the GPC-graph represents a local cube in GPC while each edge between two adjacent nodes indicates the gluing of corresponding cubes. Figure 1(e) visualizes a typical GPC-graph. In each node (which represents a cube primitive), we have six boundary faces, which are arranged for better visualization: the middle square corresponds to the top face in the (u, v, w) parametric domain. A face could be glued to a part of another face, namely, cubes could have different sizes (see Section II-B). When two cubes are glued via certain faces, the graph generates an edge (gray link) between them, and a transition function must then be formulated to enable the subsequent spline construction. A critical issue is the orientation to glue the shared face and this dictates the transition function that actually bridges between local cube domains. Corresponding faces from different cubes can be properly glued with the help of arrows, indicating the gluing orientation.

B. Partial Gluing

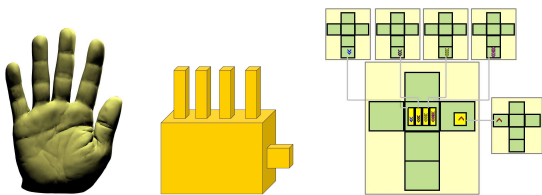


Figure 2: Parameterizing the hand model to GPC with Partial Gluing. From left to right: the original model, its GPC, and the GPC graph.

Conventional PC typically consists of cubes of uniform size, hence each cube face glues to another cube face in its entirety. This limits the valence of a cube cell to six. It is more flexible to allow the size of cubes to be non-uniform and a small cube can be glued to a part of a face of a big cube. Adjacent sub-regions with different solid volumes

can then be parameterized to two cubes of different sizes, guaranteeing coherent parameterization. For example, in Fig. 2, cubes of fingers are partially glued to the cube of the palm. The parameterization and gluing are also clearly illustrated on the GPC-graph. In the interest of space, we refer interested readers to [5] for more implementation details on partial gluing.

C. GPC Construction and Parameterization

Given a solid model as a general input, the GPC-graph and GPC parameterization can be computed simultaneously in the following procedure:

1. **Topological Decomposition.** Partition the model to several components so that each component has trivial topology. A homology basis of a closed genus- g surface can be computed automatically [1], and the surface can be canonically decomposed into a set of $2g - 2$ pants patches [6]. The volumetric primitive bounded by each pants patch can be further decomposed into four topological cubes.

2. **Geometric Decomposition.** For each volumetric primitive, detect long and thin branches using the shape skeleton [11], then remove each long branch and parameterize it to a single cube domain.

3. **Cube Parameterization.** Parameterize each sub-region using a cube domain.

Intuitively, in Steps 1 and 2, each handle of the original model is parameterized to a “T”-shaped GPC, composed by four cubes. Long and thin branches (like antennae) are also parameterized to cube primitives separately. The algorithm of cube parameterization is as follows: (3.1) 8 vertices on the boundary are either selected or derived (from adjacent primitives to ensure the consistency), and they are mapped to the corners of the cube; shortest paths connecting pairs of corner vertices partition the boundary into 6 quadrilateral regions; (3.2) compute the harmonic surface map [2] for each quadrilateral region that can map to one of the cube’s faces, subject to all the curve boundary constraints; (3.3) solve the 3D Laplacian equation [12] to arrive at the interior volumetric parameterization.

III. TRIVARIATE GPC-SPLINES

A. Point-Based Splines

Tensor-product trivariate B-splines are usually defined over the parametric cube domain. In order to allow hierarchical and adaptive fitting, without significantly increasing the number of control points, T-splines (that allows T-junctions for knots and control points) have been proposed [8]. T-splines are point-based splines whose control

points form a T-mesh and have no regular connectivity with surrounding ones. In this paper, as a natural generalization of our work of designing bivariate T-splines on Polycube surface domain [10], our ambitious goal is to design the trivariate T-splines over GPC for general volumetric data. We shall highlight the idea of our spline construction by fitting C^2 -continuous parametric solid, while generalizing it to globally C^n -continuous representation is straightforward.

Each control point C_i (located in parametric cube D^j with local coordinate \mathbf{c}_i^j) is associated with three knot vectors along three principal axis directions: $r = [r_1, r_2, r_3, r_4, r_5]$, $s = [s_1, s_2, s_3, s_4, s_5]$, $t = [t_1, t_2, t_3, t_4, t_5]$, where $r_3 = 0$, $s_3 = 0$, and $t_3 = 0$. For any sample point with (u, v, w) as its parameter, the blending function is

$$B_i(u, v, w) = N_r(u) \times N_s(v) \times N_t(w), \quad (1)$$

where N_r , N_s , and N_t are cubic B-spline basis functions associated with the knot vector r , s , and t respectively. The formulation for a PB-spline on this point is

$$P(u, v, w) = \frac{\sum_0^n C_i B_i(u, v, w)}{\sum_0^n B_i(u, v, w)}. \quad (2)$$

By parameterizing the solid model to a GPC, PB-splines defined on cubes can achieve a globally continuous representation for any input model. The global parametric domain is equivalent to a collection of coordinate charts in all constituting local cube primitives via cube parameterization, and these local charts are then glued coherently to form the entire GPC parametric domain, enabled by the GPC-graph. As a result, the global PB-splines are piecewise rational polynomials defined on GPC, whose transition functions between adjacent cube primitives are compositions of translations and rotations of $n\pi/2$. Note that unlike the PolyCube surface splines, trivariate splines defined on GPC do not have singularities in solid interior.

Given an arbitrary parameter \mathbf{u} in cube D^j (also denoted as \mathbf{u}^j), the spline approximation can be carried out as follows:

- (1) Find all the neighboring cubes $\{D^i\}$ that support \mathbf{u} (i.e., it contains control points C_k that may support \mathbf{u});
- (2) The spline function is:

$$P(\mathbf{u}) = \frac{\sum_{k=0}^n C_k^i B_k(\phi^{ij}(\mathbf{u}^j) - \mathbf{c}_k^i)}{\sum_{k=0}^n B_k(\phi^{ij}(\mathbf{u}^j) - \mathbf{c}_k^i)}, \quad (3)$$

where \mathbf{u}^j is the local parametric coordinate of point \mathbf{u} in the cube domain D^j , ϕ^{ij} is the transition function from cube domain D^j to D^i , C_k^i denotes the control point k in the cube domain D^i , and \mathbf{c}_k^i is its local coordinate.

The transition function ϕ^{ij} from cube domains D^j to D^i is a composition of translations and rotations following the consecutive path where we glue cube D^j to cube D^i . In the GPC-graph, if we assign the weight on each edge $[D^i, D^j]$ to be the length of the translation vector that transforms one local frame to the other, then this transition function can be easily derived by navigating through the shortest path $\widehat{D^i D^j}$ from node D^i to D^j .

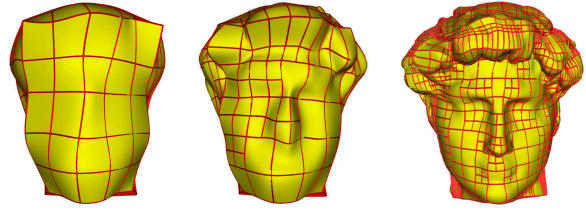


Figure 3: Hierarchical spline fitting results at levels 0, 1, and 2, respectively.

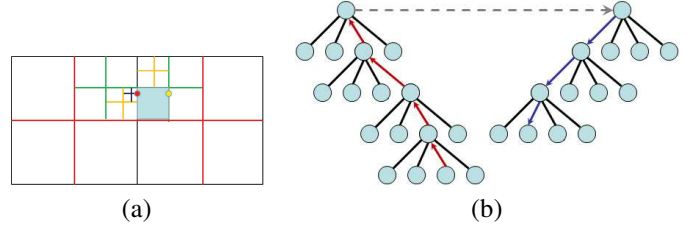


Figure 4: Knots Traversal illustrated on a quad-tree.

Suppose $\widehat{D^i D^j} := D_1 (= D^i) \rightarrow D_2 \dots \rightarrow D_n (= D^j)$, and the transition function $\Phi_{(i,i+1)}$ (derived by way of cube-gluing) from D_{i+1} to D_i is known, then ϕ^{ij} is formulated by

$$\mathbf{u}^i = \phi^{ij}(\mathbf{u}^j) = \Phi_{1,2}(\Phi_{2,3}(\dots \Phi_{n-1,n}(\mathbf{u}^j))).$$

B. Hierarchical Fitting

A key advantage for defining T-splines upon GPC is that the evaluation of each node relies on just a union of general cubes in nearby regions. Moreover, the hierarchical fitting and level-of-detail control can be efficiently developed, which have two attractive properties: eliminating a large percentage of superfluous control points by introducing T-junctions; and providing adaptive control to users for properly balancing between fitting accuracy and efficiency.

The spline fitting is defined as follows. We have the parameterized solid model being generated from the boundary representation. The sample point in the model is $f(\mathbf{u}_i)$, where \mathbf{u}_i is the parametric coordinate for each sample point. We minimize the following equation:

$$E_{dist} = \sum_{i=0}^n \|P(\mathbf{u}_i) - f(\mathbf{u}_i)\|^2, \quad (4)$$

where $P(\mathbf{u}_i)$ is the approximation of each sample point acquired from Eq. (3). Given a sample parametric point \mathbf{u} in GPC, we measure the root-mean-square error (rms) $\sigma(\mathbf{u})$ between its spatial position $f(\mathbf{u})$ and its spline approximation $P(\mathbf{u})$.

In each cube domain, we start from a coarse representation, denoted as T-mesh H_0 , and assign a control point for each vertex. Then from level k to level $k+1$, a cell on H_k is subdivided into 8 sub-cells in H_{k+1} if the fitting error of this cell is larger than a given tolerance. The cell fitting error is the maximal error $\sigma(\mathbf{u})$ of sample points \mathbf{u} in this cell. Algorithm 1 offers a high-level sketch for the hierarchical fitting procedure.

Algorithm 1 Hierarchical Spline Fitting

```

for all cube domain  $D_i$  do
  Initialize  $H_0^i$  and control points,  $k = 0$ 
end for
loop
  1. Traverse and get knot vectors for all control points.
  2. Evaluate  $P(u)$  in Eq.(3) for all sample points.
  3. Spline Fitting: Minimize  $E_{dist}$  in Eq.(4).
  4. Compute the fitting error of each cell:
  for all cells  $H_j^k$  in level  $k$  do
    if  $\text{Error}(H_j^k) \geq \text{tolerance}$  then
      Subdivide  $H_j^k$  and add new control points.
    end if
  end for
  if No cell is subdivided then
    Stop.
  end if
   $k = k + 1$ 
end loop

```

C. Implementation based on Octree Structure

Traversing Knot Vectors. We use the method of “Ray-Traversing” [8] to generate 3 knot vectors for each control point. Unlike surface splines, enabling T-junctions in volumetric domains can result in much more complicated data structure and very time-consuming knot computation. We implement the octree data structure for efficient knots traversing. However, we restrict that a cube can only be divided to 8 sub-cells of equal size during refinement (note that, originally [8] allowed dividing a cell to 2 or 4 cells of different sizes, which becomes extremely complicated in 3D), because it greatly reduces the implementation complexity and improves the efficiency of knots traversing.

In Fig. 4, we only highlight our idea for efficient knots traversal in a 2D layout using quad-trees. This idea can be directly generalized to 3D using octrees. In a quad-tree, let L, R, T, and B denote the current cell that locates at the left, right, top, and bottom (in 3D, also front and back) w.r.t. its parent cell, respectively. In (a), suppose we traverse a ray starting from the red point (on cell C_s) to right, and need to know the cell C_t that contains the yellow point on its right face (because once we have C_t , the knots vector can be computed directly). The first step is to locate the smallest common ancestor C_{st} (or up to level-0, the GPC-graph) of cells C_s and C_t . C_s and its parent cells should be always on the “Right” of their parent cells. This is because once it becomes a “Left” cell, that parent cell is the smallest common ancestor C_{st} . The path from C_s to C_{st} , as the red path shown in (b), can be encoded as a string $T_s = \{RT, RB, RT, RT\}$. The path from C_{st} to C_t can be efficiently traced by first reversing T_s (to $\{RT, RT, RB, RT\}$), then replacing all R with L (because we are traversing towards right), resulting in the encoding $T_t = \{LT, LT, LB, LT\}$. T_t indicates the traversal from C_{st} to C_t , plotted as the blue path in (b). More implementation details can be found in [5].

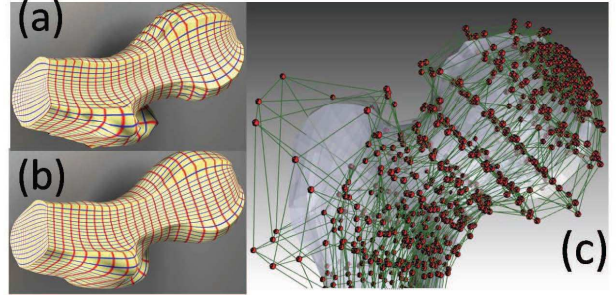


Figure 5: Volumetric T-spline representation of the Femur model. (a) The volumetric parameterization; (b) the spline fitting result; (c) the zoom-in structure of control points.

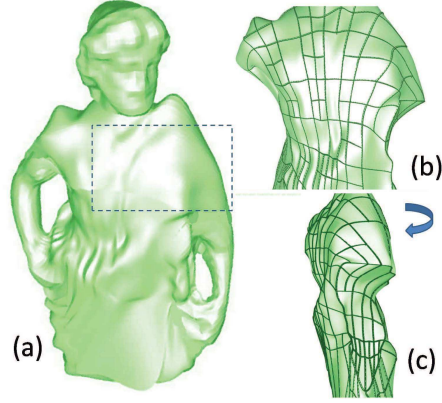


Figure 6: Splines for the Solid Greek. (a) The fitting result; (b,c) the T-junction on the surface and on the cross-section.

IV. EXPERIMENTAL RESULTS

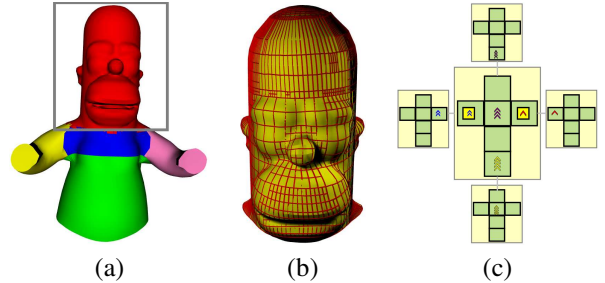


Figure 7: T-splines for the Solid Homer Model. (a) The fitting result; (b) the zoom-in of head with T-meshes; (c) GPC-graph.

Model	Bimba	Femur	Kitten	Greek	Homer
S #	25,000	12,250	40,000	31,300	22,400
C #	1,905	1,430	2,304	4,365	3,070
rms (avg)	0.096%	0.077%	0.35%	0.53 %	0.21%

Table I: Spline Construction Runtime Table. The $S\#$, $C\#$, and rms are the number of sample points, control points, and the average rooted mean square errors, respectively.

We demonstrate the efficacy of our framework by converting several solid models into trivariate spline representations. Fig. 5 shows the spline representation of a solid Femur model. Its GPC parameterization is shown in (a), the fitted T-spline result is illustrated in (b), and the control point structure is visualized in (c). Fig. 6 shows the spline representation of the solid Greek model whose

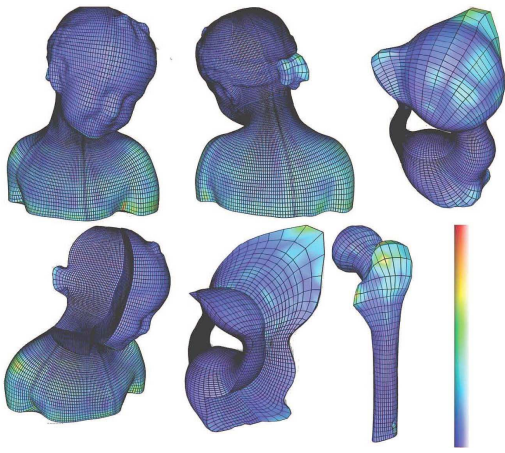


Figure 8: The spline fitting error of Kitten, Bimba, and Femur models. The fitting error is color-coded from blue (minimum) to red (maximum).

Property	GPC	PC	Cylinder [7]	SC [3]
Regularity	Yes	Yes	Singularity	No
C-Valence	n	6	2	n
Hierarchy	Easy	Easy	Hard	Easy
Automatic Decomposition	Easy	Not Easy	Hard	Hard

Table II: Comparison of Different Parametric Domains.

boundary surface is of genus-4. (a) shows the fitting result; (b) shows the hierarchical T-junctions on the model’s boundary surface, and (c) illustrates the side view from the right arm, highlighting the interior fitting result with T-junctions. Fig. 7 illustrates the T-spline representation of the Homer model. (a) is the global fitting result, (b) zooms in the head region with T-junctions illustrated, and (c) shows its GPC-graph.

Fitting errors (rooted mean square errors, with models normalized to a unit box) on several models are color-encoded and illustrated in Fig. 8. The statistical results are given in Table I. In most of our experiments, approximation with good quality can be obtained after 3 iterations of hierarchical refinement.

A **comparison** among GPC and some other parametric domains is given in Table II. The grid structures of GPC, PC, and Cylinder domains are orthogonal. In cylindrical parameterization [7], the central line is singular, and on PC or GPC parameterization there is no singularity point. These three parameterizations have regular control nets, leading to simple and efficient evaluations, in contrast, simplicial complex splines are built upon irregular triangular structures. Each cell of PC has up to six adjacent cells and cylindrical cell can have at most two adjacent cells, these limit the way that different sub-regions can connect and increase the difficulty of designing effective decomposition on general models. Simplicial complex splines do not have such a limitation, and by allowing non-uniform sized cubes, GPC also has the flexibility to glue many cubes. Simplicial complex supports local subdivision easily, while for regular structures such as cylinders, this is difficult. By allowing T-junctions, PC and GPC afford efficient hierarchical refinements as well.

V. CONCLUSION

We have presented a global “one-piece” trivariate hierarchical spline construction framework based on Generalized PolyCube (GPC) parameterization. The GPC concept enables a novel and desirable mechanism that facilitates the “one-piece” spline representation. We have articulated the decomposition and parameterization procedure. Global trivariate T-splines can be constructed on GPC and transition functions can be effectively computed using the GPC-graph. The entire spline construction framework affords hierarchical refinement and level-of-detail control. Our GPC trivariate T-splines have great potential in various shape design and physical analysis applications.

ACKNOWLEDGMENTS

This work is supported in part by NSF IIS-0949467, NSF IIS-0710819, Louisiana Board of Regents RCS LEQSF(2009-12)-RD-A-06, and PFund: NSF(2009)-PFUND-133.

REFERENCES

- [1] T. Dey, K. Li, and J. Sun. On computing handle and tunnel loops. pages 357–366. International conference on cyber worlds, 2007.
- [2] M. Floater. Mean value coordinates. *Comput. Aided Geom. Des.*, 20(1):19–27, 2003.
- [3] J. Hua, Y. He, and H. Qin. Multiresolution heterogeneous solid modeling and visualization using trivariate simplex splines. pages 47–58. Proc. ACM Symp. on Solid Modeling and Applications, 2005.
- [4] T. Hughes, J. Cottrell, and Y. Bazilev. Isogeometric analysis: Cad, finite elements, nurbs, exact geometry and mesh refinement. *Computer Methods in Applied Mechanics and Engineering*, 194:4135–4195, 2005.
- [5] B. Li, X. Li, and H. Qin. Generalized polycube construction and parameterization. *Technical Report*, www.cs.sunysb.edu/~bli/volumeparam.pdf, 2010.
- [6] X. Li, X. Gu, and H. Qin. Surface mapping using consistent pants decomposition. *IEEE Trans. on Visualization and Computer Graphics*, 15(4):558–571, 2009.
- [7] T. Martin, E. Cohen, and R. Kirby. Volumetric parameterization and trivariate b-spline fitting using harmonic functions. *Comput. Aided Geom. Des.*, 26(6):648–664, 2009.
- [8] T. Sederberg, J. Zheng, A. Bakenov, and A. Nasri. T-splines and t-nurccs. *ACM Trans. Graph.*, 22(3):477–484, 2003.
- [9] M. Tarini, K. Hormann, P. Cignoni, and C. Montani. Polycube maps. *ACM Trans. Graph.*, 23(3):853–860, 2004.
- [10] H. Wang, Y. He, X. Li, X. Gu, and H. Qin. Polycube splines. *Computer Aided Design*, 40(6):721–733, 2008.
- [11] H. Wang, Y. He, X. Li, X. Gu, and H. Qin. Geometry-aware domain decomposition for t-spline-based manifold modeling. *Comput. Graph.*, 33(3):359–368, 2009.
- [12] K. Zhou, J. Huang, J. Snyder, X. Liu, H. Bao, B. Guo, and H.-Y. Shum. Large mesh deformation using the volumetric graph laplacian. *ACM Trans. Graph.*, 24(3):496–503, 2005.